PHYSICAL REVIEW C **88**, 051303(R) (2013)

# Switch from short-axis to intermediate-axis rotation in $^{138}$Nd

C. M. Petrache,[1] I. Ragnarsson,[2] Hai-Liang Ma,[3] R. Leguillon,[1] T. Konstantinopoulos,[1] T. Zerrouki,[1] D. Bazzacco,[4] and S. Lunardi[4]

[1]*Centre de Sciences Nucléaires et de Sciences de la Matière, Université Paris-Sud and CNRS/IN2P3, Bâtiment 104-108, F-91405 Orsay, France*

[2]*Division of Mathematical Physics, LTH, Lund University, Post Office Box 118, SE-221 00 Lund, Sweden*

[3]*Department of Nuclear Physics, China Institute of Atomic Energy, Box 275(10), Beijing 102413, China*

[4]*Dipartimento di Fisica e Astronomia dell'Universita and INFN Sezione di Padova, I-35131 Padova, Italy*

(Received 4 February 2013; revised manuscript received 27 September 2013; published 13 November 2013)

It is pointed out that the triaxial bands in $^{138-140}$Nd and in the Lu/Er nuclei can be understood from the same shell structure effects. Two of the bands in $^{138}$Nd, interpreted as signature partners, exhibit a crossing at high spins with a signature splitting which is strongly reduced above the crossing. This behavior is unique among the yrast and close-to-yrast configurations, revealing the mechanism which induces a change of the rotation axis from short to intermediate in the triaxially deformed nucleus.

DOI: 10.1103/PhysRevC.88.051303 PACS number(s): 21.10.Re, 21.60.Ev, 23.20.Lv, 27.60.+j

The existence of triaxially deformed nuclei is a long-standing debate. There exist numerous papers where triaxiality in nuclear ground states and at small angular momenta are suggested. However, the corresponding minima in the energy surfaces are generally soft [1], and it appears questionable how well the nonaxial shape is stabilized. Indeed, it is mainly for higher-spin states, where the special symmetries associated with (static) axially symmetry are severely broken, that triaxial shape is clearly defined. This is the case for the smooth terminating bands [2,3] which develop over triaxial shape with increasing spin. At the highest spins the shape becomes axially symmetric with the rotation around the symmetry axis, as supported for example by lifetime measurements in the $A = 110$ region [4]. More recently, rotational high-spin bands in Nd nuclei with $A = 138$–$140$ have been identified [5–8], with an $\mathcal{J}^{(2)}$ moment of inertia (defined from the differences in the $E_\gamma$ energies) which is less than half of the rigid body value. Such bands can only be formed at triaxial shape, where they are well understood from configurations with well-developed minima at $\varepsilon_2 \approx 0.25$, $\gamma \approx 35^\circ$, where the deformation of the nucleus is specified by $\varepsilon_2$ and $\gamma$; see, e.g., Ref. [3]. For $\gamma = 0^\circ$, the nucleus is prolate with a quadrupole moment $Q_{20} \approx (4/5)Zr_0^2A^{2/3}\varepsilon_2(1 + \varepsilon_2/2)$ ($r_0$ is the radius parameter, $r_0 \sim 1.2$ fm) [10]. The triaxiality is specified by $\gamma$, where $\gamma > 0^\circ$ corresponds to rotation around the shortest principal axis (largest rigid-body moment of inertia) according to the Lund convention [11]. The transitional quadrupole moment is then in lowest order obtained as $Q_t = Q_{20}\cos(\gamma + 30^\circ)/\cos(30^\circ)$.

Compared with the Nd bands, an even more convincing fingerprint of triaxiality at high spins is the existence of wobbling bands, which have been discovered in the odd-even Lu isotopes [12] and understood as formed at a triaxial shape with $\varepsilon_2 \approx 0.30$, $\gamma \approx 20^\circ$. It is now of special interest that somewhat similar bands have been discovered in nuclei with a few particles less than $^{163}$Lu, namely $^{157,158}$Er [13] and neighboring nuclei; see, e.g., Refs. [14,15]. The bands in the Er isotopes first appeared to be well understood as based on similar configurations as those in the Lu isotopes. However, subsequent lifetime measurements [16,17] showed that the transition probabilities were larger than expected, suggesting that these bands are based on a larger deformation, or, alternatively, are rotating around the intermediate axis corresponding to a negative value of $\gamma$. The preferred rotation axis is still an open issue, although most calculations [16,18–20] suggest that the minimum at positive $\gamma$ is lower in energy for most configurations, which would then make the minimum at negative $\gamma$ unstable towards tilting of the rotating axis [18].

In view of this debate about the triaxiality at high spins and the preferred rotational axis, the results on the bands of $^{138}$Nd reported here are of special interest. We have in fact identified two rotational bands whose properties correspond to rotation around the shorter principal axis (positive $\gamma$) at low spin and around the intermediate principal axis (negative $\gamma$) at high spin. There are two clear fingerprints of this change of the rotational axis: the calculated energies of the corresponding minima in the energy surfaces and the spin dependence of signature splitting in these signature partner bands. In particular, the observed degeneracy of the bands in the high-spin range is in agreement with general rules of signature splitting at the bottom of high-$j$ shells.

The experimental details for the present data, taken with the GAsp SPectrometer (GASP) at Legnaro National Laboratory, can be found in Ref. [21]. The two high-spin bands of $^{138}$Nd discussed in this Rapid Communication, $T1$ and $T2$, are shown in Fig. 1. They have been observed together with other 12 rotational bands, which will be reported in a separate paper [22]. In Fig. 1 we also show the transitions de-exciting the band $T1$ towards the bands $L1$, $L2$, and $L3$ and the yrast $20^+$ state [21], as well as the transitions connecting the bands $T2$ and $T1$. Doubly gated spectra for the bands are given in Fig. 2.

The bands $T1$ and $T2$ have been already reported previously [5], from an experiment performed with the $8\pi$ spectrometer. The reduced number of triple coincidences in that experiment limited the analysis to only double-coincidence events, which were not always sufficient to firmly place the transitions. The new data have much higher statistics and enabled the analysis of triple-coincidence events, which helped

 

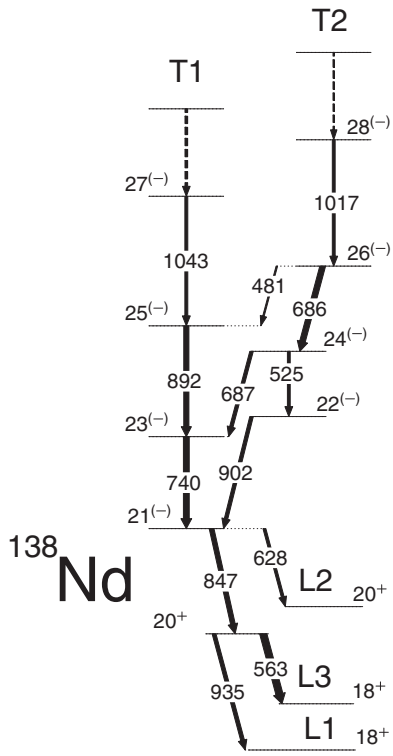


FIG. 1. Partial level scheme of $^{138}$Nd showing the lower part of the high-spin bands $T1$ and $T2$.

to solve several ambiguities in the level scheme, especially at the bottom of the bands. We could firmly identify the decay-out transitions and therefore firmly establish the spins but not the parity of the bands.

Band $T1$ is the second strongest populated high-spin band in $^{138}$Nd with a relative intensity of 15% and decays towards the bands $L1$, $L2$, and $L3$ and the yrast $20^+$ state as shown in Fig. 1. Band $T2$ has an intensity of 7% and decays to band $T1$ and towards a possible cascade from which we observed only the 525-keV transition. We confirm all transitions of bands $T1$ and $T2$ observed previously [5]. The band $T1$ is extended by

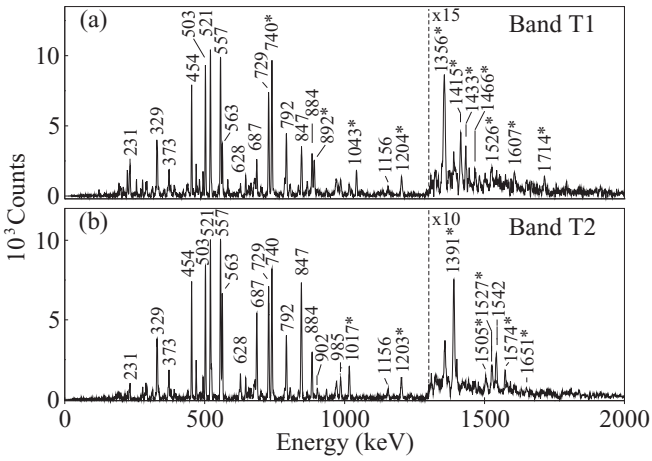


FIG. 2. Double-gated sum spectra for the bands $T1$ and $T2$ in $^{138}$Nd. The gates were set on selected transitions of each band. The transitions marked with asterisks represent the members of the band.

six more transitions of 1415.0, 1433.2, 1466.1, 1525.6, 1607.4, and 1714.4 keV up to spin 43, and band $T2$ is extended by four more transitions of 1574.4, 1526.9, 1505.2, and 1651.2 keV up to spin 42, ordered by decreasing intensity. However, several changes were necessary at the bottom of the bands, which lead to different energy assignments than those reported in Ref. [5].

The spin-parity assignments are based on DCO (directional correlation of oriented states) ratios, which in the present experiment are expected to be 0.5 for pure $\Delta I = 1$ transitions and 1 for $\Delta I = 2$ transitions when gating on $\Delta I = 2$ transitions. The DCO ratios of the 847- and 628-keV transitions de-exciting band $T1$ are 0.43(20) and 0.74(25), respectively, being in agreement with either $M1$ or $E1$ character. These values fix the spin of the lowest state of band $T1$ at $21\hbar$, while the parity is uncertain. The DCO ratios of the 481- and 687-keV transitions de-exciting band $T2$ are 0.76(15) and 0.93(20), respectively, which are in agreement with $M1/E2$ and $E2$ character, respectively. We could also extract the DCO ratios of 1.03(26) for the 525-keV transition and 0.61(15) for the 902-keV transition, which are in agreement with $E2$ and $M1/E2$ character, respectively. These values fix the spin of the lowest observed state of band $T2$ at $26\,\hbar$. The parity of the band is the same as that of band $T1$, since the connecting transitions to band $T1$ are of $M1/E2$ character, which do not change the parity. Based on theoretical interpretation given below, we assign negative parity to both bands $T1$ and $T2$.

Collective high-spin bands are generally analyzed using the cranking model [23]. These calculations can be carried out to varying degree of sophistication, for example, using the traditional approach of directly postulating a parameterized mean-field potential such as a Nilsson potential [11,24] or by postulating a density functional [25] which then gives rise to a corresponding potential. With carefully fixed parameters, these different approaches will give essentially the same result. For example, calculations based on the modified oscillator and the relativistic mean field are compared in Refs. [9,26]. Furthermore, Skyrme-Hartree-Fock calculations and Nilsson-type calculations give similar results for the triaxial bands in Er nuclei [13,16,18].

In the analysis of the $T1$ and $T2$ bands in $^{138}$Nd, it is crucial to be able to fix configurations and follow them also for spin values when they are not yrast. Methods to do this were introduced in calculations using the modified oscillator long ago [2,24]. However, to our knowledge, no methods to follow rotational bands in a similar way has been reported with any other mean field approach. Therefore, in our analysis we use the cranked Nilsson-Strutinsky (CNS) formalism [3,24,27], which is based on the modified oscillator potential. However, we get a general understanding of the bands in terms of the alignment of the orbitals dominated by specific $j$ shells. Thus, we are convinced that our results have a wider applicability; i.e., they can be considered as the typical outcome of a cranked mean field approach. In the calculations we use the so-called $A = 150$ parameters [28], in line with other recent investigations of the high-spin states in this region of nuclei [7,8,29].

Before discussing the interpretation of the $T1$ and $T2$ bands in $^{138}$Nd, we analyze some specific features which lead to triaxial shapes. The triaxial bands in $A \approx 155$–$170$ nuclei

and those discussed here in the Nd isotopes have a common origin [30]: all these bands are formed in configurations with two (or possibly three or four) holes in the $\mathcal{N} = 4$, $n_z = 0$ orbitals. It is the interaction between these orbitals which induces the triaxial shape as illustrated at the deformation of the $A \approx 155$–$170$ bands in Fig. 4 of Ref. [13]. An analogous diagram can be drawn at the smaller deformation of the Nd bands. Furthermore, the triaxial bands observed in $^{142}$Gd have similar configurations [29] as the $^{138-140}$Nd bands but with the difference that no neutron is excited to the $j$ shells above the $N = 82$ gap. Finally, the same mechanism but in the $\mathcal{N} = 4$, $n_z = 1$ orbitals has been invoked to explain why $^{126}$Pr$_{67}$ appears to be triaxially deformed in contrast to $^{128}$Pr$_{69}$ [31].

A different mechanism leading to triaxial shape is active when particles at the bottom of a high-$j$ shell align their angular momenta along the rotational axis. They can thus be understood as having their matter distribution in a plane perpendicular to the rotation axis, trying to polarize a prolate nucleus towards triaxial shape, rotating around the shortest principal axis ($\gamma > 0°$) [32]. In terminating bands where many such high-$j$ particles align, such effects lead to a strong driving force towards triaxial and finally oblate shape [3]. One should also note that holes in the orbitals at the top of a high-$j$ shell will have the opposite driving force, i.e., towards $\gamma < 0°$ [32].

In the $^{138-140}$Nd nuclei, both these types of driving forces towards triaxial shapes are present. The interaction between the $\mathcal{N} = 4$, $n_z = 0$ orbitals are to first order independent of the rotational axis; i.e., there is no specific preference for the sign of $\gamma$, while the alignment of several high-$j$ particles will polarize the nucleus towards $\gamma > 0°$. Therefore, the triaxial bands in these nuclei show a very clear preference for rotation around the shorter principal axis, but as demonstrated below, in specific cases with only a few aligning high-$j$ orbitals, rotation around the intermediate axis ($\gamma < 0°$) might be observed.

When comparing observed and calculated rotational bands, it is advantageous to plot them relative to a rotating liquid drop reference; see Ref. [27]. The observed bands $T1$ and $T2$ will then come out as in Fig. 3(a). The pronounced curvature seen for $I \approx 20$–$35$ is typical for the triaxial bands in this region. This curvature is directly related to the small values of the $\mathcal{J}^{(2)}$ moment of inertia.

The triaxial bands in the Nd nuclei are characterized by having one or several neutrons excited across the $N = 82$ gap to the $h_{9/2}f_{7/2}$ and $i_{13/2}$ orbitals [5]. They can thus be specified from the dominating amplitudes of hole and particle states relative to a $^{132}$Sn core,

$$\pi(h_{11/2})^{p_1}\nu(h_{11/2})^{-n_1}(h_{9/2}f_{7/2})^{n_2}(i_{13/2})^{n_3}$$

or in short $[p_1, n_1(n_2n_3)]$. For $^{138}$Nd ($Z = 60$, $N = 78$), the number of $d_{5/2}g_{7/2}$ protons and $d_{3/2}s_{1/2}$ neutron holes is then $10 - p_1$ and $4 + n_2 + n_3 - n_1$, respectively.

It has been shown previously that the minimum of the $E - E_{rld}$ curves is directly related to the maximum spin contribution from the high-$j$ particles [6] or even more simply, from the number of high-$j$ particles, i.e., to $(p_1 + n_2 + n_3)$. With the minimum at $I \approx 27$ for the $T1$ and $T2$ bands, we can then conclude that they should most likely be assigned to configurations with four high-$j$ particles. Combining all

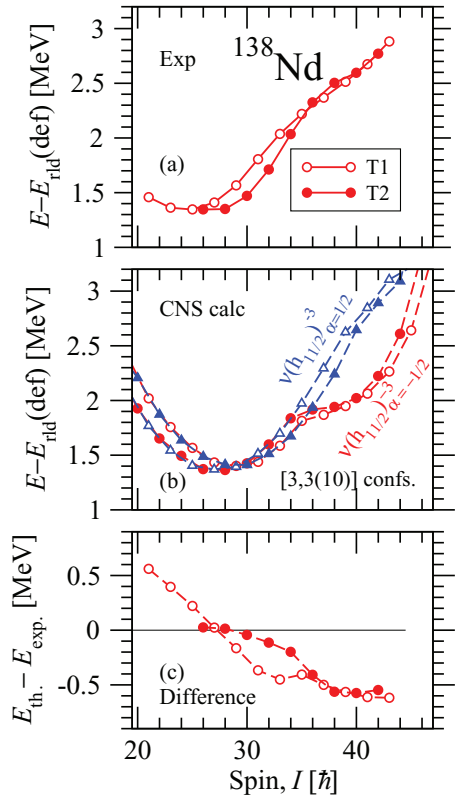


FIG. 3. (Color online) The observed bands $T1$ and $T2$ and the configurations assigned to them are drawn relative to the rotating liquid drop reference in the upper and middle panels, respectively, with their difference in the lower panel. In the middle panel, also the neutron $h_{11/2}$ signature partners are drawn. Note that with the Fermi surface in the upper region of the $h_{11/2}$ shell, signature degeneracy is calculated for $\gamma \approx 30°$ and a large signature splitting for $\gamma \approx -30°$, while the $h_{9/2}f_{7/2}$ particle at the bottom of the shell leads to signature degeneracy for $\gamma \approx -30°$, but because of the mixture of two $j$ shells, there is only a small signature splitting for $\gamma \approx 30°$.

reasonable proton and neutron configurations, those with four high-$j$ particles and negative parity are drawn in Fig. 4. It is then mainly configurations of the type [3,3[10)] which have the minimum around $I \approx 27$. Possible alternatives might be [2,2(11)] or [2,3(20)] and, because the parity of the observed bands is not determined, also the positive-parity configurations with four high-$j$ particles must be considered. However, taking into account also the band crossing at $I \approx 35$, it appears that the $T1$ and $T2$ bands must be assigned to a [3,3[10)] configuration. In the [3,3(10)] bands there is an odd number of particles in the proton and neutron $h_{11/2}$ shells, as well as in the proton $d_{5/2}g_{7/2}$ shells and the neutron $h_{9/2}f_{7/2}$ shells. In general, low-lying configurations might then be formed for both signatures of the odd particle; i.e., there are $2^4 = 16$ such configurations. However, the yrast minimum is generally found for $\gamma > 0°$ deformation as concluded already in Ref. [5]. For such shapes, the configurations with the unfavored signature, $\alpha = 1/2$, of the odd $h_{11/2}$ proton are high in energy (not shown in Fig. 4). Furthermore, the configurations with $\alpha = 1/2$ for the $d_{5/2}g_{7/2}$ protons (drawn by squares in Fig. 4) are clearly higher in energy than those with $\alpha = -1/2$ (drawn

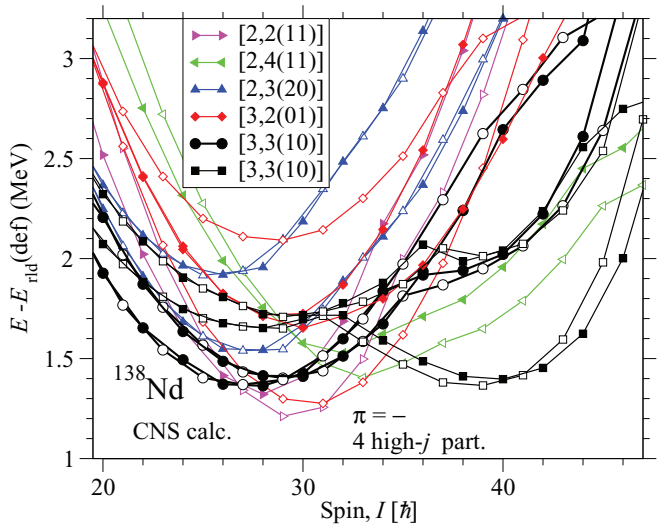


FIG. 4. (Color online) Calculated energies of negative-parity configurations with four high-$j$ particles are shown relative to the standard rotating liquid drop reference. Closed (open) symbols are used for signature $\alpha = 0$ ($\alpha = 1$), with the labels explained in the text.

by circles). The latter, which are lowest in energy in the spin range $I \approx 25$–$30$, are drawn in the middle panel of Fig. 3. They have the same signature for the proton orbitals but differ by the signature of the neutron $h_{11/2}$ and $h_{9/2}f_{7/2}$ orbitals. The configurations with signature $\alpha = -1/2$ for the odd $h_{11/2}$ neutron go through a shape change from positive $\gamma$ to negative $\gamma$ at $I \approx 35$, resulting in an equilibrium shape of $\varepsilon_2 \approx 0.15$, $\gamma \approx -30^\circ$ at high spin as illustrated in the middle panel of Fig. 5. The corresponding band crossing seen in Fig. 3 is in nice agreement with the band crossing observed in the $T1$ and $T2$ bands (upper panel of Fig. 3). The detailed configurations assigned to these observed bands can be written as

$$\pi(d_{5/2}g_{7/2})^{7}_{11.5}(h_{11/2})^{3}_{13.5}$$
$$\nu(d_{3/2}s_{1/2})^{-2}_{2}(h_{11/2})^{-3}_{13.5}(h_{9/2}f_{7/2})^{1}_{3.5,4.5},$$

where the maximal spin values in the different groups is given as subscript from which also the signature of the odd particle can be read out. Using the same standard formulas as in Ref. [16], the calculated transitional quadrupole moment

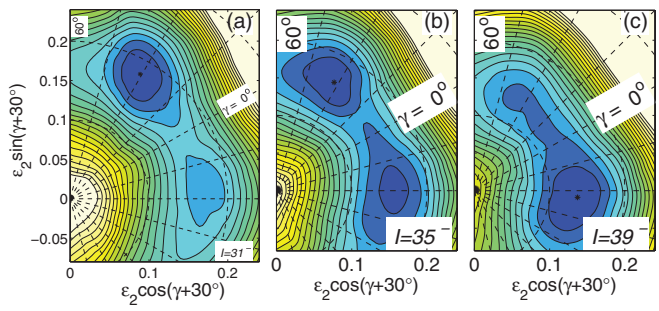


FIG. 5. (Color online) Calculated potential energy surfaces in the $(\varepsilon_2, \gamma)$ plane, illustrating the shape change around $I = 35$ for the [3,3(10)] configuration assigned to the $T1$ band. The contour line separation is 0.25 MeV.

$Q_t$ jumps from $Q_t \approx 2$ eb just before the crossing to $Q_t \approx 3$ eb just after the crossing. Thus, the shape changes predicted here can be tested if the $B(E2)$ transition probabilities are measured up to high spin values.

With the bands $T1$ and $T2$ assigned to these [3,3(10)] configurations, the difference between experiment and calculations comes out as in the lower panel of Fig. 3. The general appearance of this difference is consistent with what is expected from the neglect of pairing correlations, i.e., that the difference comes rather close to zero and increases with decreasing spin in line with the expected increase of the pairing correlations, which become stronger at lower spins. Thus, we have also carried out calculations in the Cranked Nilsson-Strutinski Bogoliubov (CNSB) formalism [29] with a self-consistent treatment of the pairing correlations, but where configurations can only be fixed by the total parity and signature for protons and neutrons, respectively. By comparing the paired and unpaired calculations, an $I$ dependence of the average pairing can be estimated. If this average pairing is added to the calculated CNS energies, the differences in the lower panel of Fig. 3 will be close to constant, giving strong support to the present assignment.

The two configurations assigned to the $T1$ and $T2$ bands have different signatures for the $h_{9/2}f_{7/2}$ neutrons, which explains why the two bands become signature degenerate above the crossing. In fact, according to general rules in high-$j$ shells, signature degenerate bands are formed at the top of the shell at prolate shape and at the bottom of the shell at oblate shape [33]. The generalization to triaxial shape was first considered by Meyer-ter-Vehn [34] and is most easily read out from a diagram where the single-particle orbitals are drawn as a function of $\gamma$ at a finite rotational frequency; see Fig. 14 of Ref. [35]. From such a diagram one can read out that the lowest orbital in a high-$j$ shell (in this case a mixed $h_{9/2}f_{7/2}$ shell) is signature degenerate from $\gamma \approx -30^\circ$ over oblate shape at $\gamma = -60^\circ$, etc. Consequently, with a calculated deformation of $\gamma \approx -30^\circ$ above $I \approx 35$, see Fig. 5, this general rule explains the observed signature degeneracy above $I \approx 35$ for the bands $T1$ and $T2$.

As the configurations assigned to the $T1$ and $T2$ bands (drawn with red [gray] circles in Fig. 3) have an odd number of neutron holes in the high-lying orbitals of the $h_{11/2}$ subshell, signature degenerate partners are calculated in the $\gamma = 30^\circ$–$40^\circ$ minimum, i.e., for $I \approx 20$–$35$. The partners with signature $\alpha = +1/2$ for the $h_{11/2}$ holes (drawn with blue [gray] triangles in Fig. 3) are very unfavored energetically for $\gamma < 0^\circ$. Therefore, they will not go through the shape change at $I \approx 35$. This means that for values around $I = 40$, they are much higher in energy than the configurations assigned to the observed bands which have signature $\alpha = -1/2$ for the $h_{11/2}$ holes. They are thus much higher in energy at high spin where these bands are populated. Consequently, it is not unexpected that they have not been observed. One may also note that the details of the observed signature splitting for the $T1$ and $T2$ bands below $I = 35$ is not reproduced in the present calculations. However, with two $j$ shells $f_{7/2}$ and $h_{9/2}$ involved, this splitting will depend on the details of their mixing, which are not accurately treated in the present calculations.

In summary, we have studied the triaxial bands which have been observed in $^{138-140}$Nd, comparing them with the somewhat similar bands in the Er/Lu region. For the bands in $^{138-140}$Nd, only a general understanding has been achieved in previous studies. However, we have now identified specific fingerprints so that two bands observed in $^{138}$Nd can for the first time be assigned to fixed configurations specified by the occupation of well-defined orbitals. In particular, it is shown that these bands rotate around the shorter principal axis ($\gamma > 0^\circ$) up to $I \approx 35$, where they go through a band crossing caused by a switch of the rotational axis, so that they rotate around the intermediate axis ($\gamma < 0^\circ$) for higher spin values. The switch from short- to intermediate-axis rotation is supported by general rules governing the signature splitting in high-$j$ shells.

This work was supported by the Swedish Research Council. Useful discussions with Gillis Carlsson are acknowledged.

[1] P. Möller *et al*., At. Data Nucl. Data Tables **94**, 758 (2008).
[2] I. Ragnarsson, V. P. Janzen, D. B. Fossan, N. C. Schmeing, and R. Wadsworth, Phys. Rev. Lett. **74**, 3935 (1995).
[3] A. V. Afanasjev, D. B. Fossan, G. J. Lane, and I. Ragnarsson, Phys. Rep. **322**, 1 (1999).
[4] R. Wadsworth *et al*., Phys. Rev. Lett. **80**, 1174 (1998).
[5] C. M. Petrache *et al*., Phys. Rev. C **61**, 011305(R) (1999).
[6] C. M. Petrache *et al*., Phys. Rev. C **72**, 064318 (2005).
[7] S. Bhowal *et al*., Phys. Rev. C **84**, 024313 (2011).
[8] R. Leguillon *et al*., Phys. Rev. C **88**, 014323 (2013).
[9] A. V. Afanasjev, I. Ragnarsson, and P. Ring, Phys. Rev. C **59**, 3166 (1999).
[10] W. Nazarewicz and I. Ragnarsson, in *Handbook of Nuclear Properties*, edited by D. N. Poenaru and W. Greiner (Clarendon Press, Oxford, 1996), p. 80.
[11] G. Andersson *et al*., Nucl. Phys. A **268**, 205 (1976).
[12] S. W. Ödegård *et al*., Phys. Rev. Lett. **86**, 5866 (2001).
[13] E. S. Paul *et al*., Phys. Rev. Lett. **98**, 012501 (2007).
[14] K. Lagergren *et al*., Phys. Rev. Lett. **87**, 022502 (2001).
[15] J. Ollier *et al*., Phys. Rev. C **80**, 064322 (2009).
[16] X. Wang *et al*., Phys. Lett. B **702**, 127 (2011).
[17] J. P. Revill *et al*., Phys. Rev. C **88**, 031304(R) (2013).
[18] Y. Shi *et al*., Phys. Rev. Lett. **108**, 092501 (2012).
[19] A. Kardan, I. Ragnarsson, H. Miri-Hakimabad, and L. Rafat-Motevali, Phys. Rev. C **86**, 014309 (2012).
[20] A. V. Afanasjev, Y. Shi, and W. Nazarewicz, Phys. Rev. C **86**, 031304(R) (2012).
[21] C. M. Petrache *et al*., Phys. Rev. C **86**, 044321 (2012).
[22] C. M. Petrache *et al*. (unpublished).
[23] Z. Szymanski, *Fast Nuclear Rotation* (Oxford University Press, Oxford, 1983).
[24] T. Bengtsson and I. Ragnarsson, Nucl. Phys. A **436**, 14 (1985).
[25] M. Bender, P.-H. Heenen, and P.-G. Reinhard, Rev. Mod. Phys. **75**, 121 (2003).
[26] A. V. Afanasjev and S. Frauendorf, Phys. Rev. C **71**, 064318 (2005).
[27] B. G. Carlsson and I. Ragnarsson, Phys. Rev. C **74**, 011302(R) (2006).
[28] T. Bengtsson, Nucl. Phys. A **512**, 124 (1990).
[29] B. G. Carlsson *et al*., Phys. Rev. C **78**, 034316 (2008).
[30] S. E. Larsson, P. Möller, and S. G. Nilsson, Phys. Scr. A **10**, 53 (1974).
[31] B.-G. Dong, H.-C. Guo, and I. Ragnarsson, Phys. Rev. C **74**, 014308 (2006).
[32] S. Frauendorf and F. R. May, Phys. Lett. B **125**, 245 (1983).
[33] F. S. Stephens, Rev. Mod. Phys. **47**, 43 (1975).
[34] J. Meyer-ter-Vehn, Nucl. Phys. A **249**, 111 (1975).
[35] I. Ragnarsson, Z. Xing, T. Bengtsson, and M. A. Riley, Phys. Scr. **34**, 651 (1986).